

Ionic Liquid Character of Zinc Chloride Hydrates Define Solvent Characteristics that Afford the Solubility of Cellulose

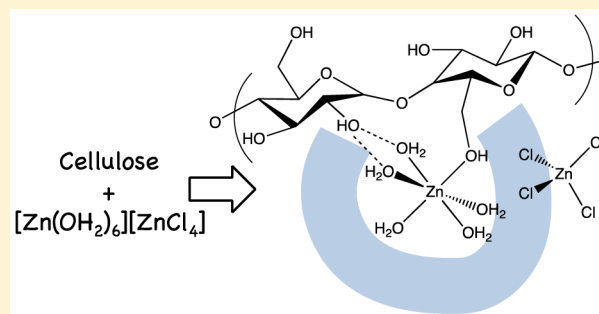
Sanghamitra Sen,^{‡,†} Bradley P. Losey,[†] Elijah E. Gordon,[†] Dimitris S. Argyropoulos,[‡] and James D. Martin^{*,†}

[†]Department of Chemistry, North Carolina State University, Raleigh, North Carolina 27695-8204, United States

[‡]Department of Forest Biomaterials, North Carolina State University, Raleigh, North Carolina 27695-8001, United States

S Supporting Information

ABSTRACT: The recently described ionic liquid structure of the three equivalent hydrate of zinc chloride ($\text{ZnCl}_2 \cdot R \text{H}_2\text{O}$, $R = 3$, existing as $[\text{Zn}(\text{OH}_2)_6][\text{ZnCl}_4]$) explains the solubility of cellulose in this medium. Only hydrate compositions in the narrow range of $3 - x < R < 3 + x$ with $x \approx 1$ dissolve cellulose. Once dissolved, the cellulose remains in solution up to the $R = 9$ hydrate. Neutron diffraction and differential pair distribution function analysis of cellulose and model compound solutions (1 wt % cellulose in the $R = 3$ hydrate and 1 wt % ethanol in the $R = 3$ hydrate and the $\text{ZnCl}_2 \cdot 3$ ethanol liquid) coupled with detailed solubility measurements suggest that cellulose solubility occurs via coordination of the primary OH to the hydrated zinc cation with ring hydroxyls forming part of a second coordination shell around the cation of the ionic liquid.



INTRODUCTION

Cellulose is one of the most abundant natural polymers. With extensive inter- and intramolecular hydrogen bonding between glycoside units of the polymer,^{1,2} it is insoluble in water and most organic solvents, dramatically restricting commercial applications despite its abundance.^{3,4} However, as described in recent reviews, this natural polymer can be dissolved in suitable solvents if the inter- and intramolecular hydrogen bonds are cleaved either by derivatization of the macromolecule or by generation of physical interactions with the solvent medium.^{3,5} Among the variety of nonderivatizing solvent systems known to dissolve cellulose, inorganic molten salt hydrates are of special interest because of their ease of preparation and recyclability. Moreover, unlike many nonderivatizing solvents, dissolution by inorganic molten salt hydrates does not require special cellulose pretreatment, which makes it both cost- and energy-efficient.^{6–13}

Inorganic molten salt hydrates are systems that have a water to salt molar ratio close to the coordination number of the strongest hydrated cation, with the water molecules being tightly bound to the inner coordination sphere of the cation.^{14,15} Reported cellulose-dissolving inorganic molten salt hydrates include $\text{LiClO}_4 \cdot 3\text{H}_2\text{O}$, $\text{LiI}_2 \cdot 2\text{H}_2\text{O}$, $\text{LiSCN} \cdot 2\text{H}_2\text{O}$, $\text{ZnCl}_2 \cdot 3\text{H}_2\text{O}$, $\text{Ca}(\text{NCS})_2 \cdot 3\text{H}_2\text{O}$, and a eutectic mixture of $\text{NaSCN}/\text{KCN}/\text{LiSCN} \cdot 3\text{H}_2\text{O}$.^{16,17} Among these, the zinc chloride hydrate is frequently used as a medium for cellulose hydrolysis and derivatization.^{17–22} Moreover, as a solvent, it is strong enough to dissolve high molecular weight bacterial cellulose.²³ The cellulose-dissolving ability of zinc chloride hydrates, $\text{ZnCl}_2 \cdot R \text{H}_2\text{O}$, strongly depends on the amount of

water present. Lu and Shen reported that when heated at 80 °C for about 2 h, the $R = 3$ zinc chloride hydrate dissolves 5.5 wt % of bacterial cellulose, but neither the $R = 2$ or 4 hydrate dissolves cellulose, though both were observed to swell the macromolecule, making a fine distribution.²³ In their efforts to synthesize 1-(furan-2-yl)-2-hydroxyethanone from cellulose hydrolysis followed by rearrangement, Yang and co-workers reported that the zinc chloride to water molar ratio influenced the product yield, increasing from 6.3 to 12.0% when the extent of hydration was changed from $R = 3.78$ to 3.36, keeping the other reaction conditions constant.²¹ The increase in the yield of the product was reported likely due to the better dissolution of cellulose in the solvent with higher concentration of zinc chloride. However, further concentration to the $R = 3.03$ hydrate was found to reduce the yield to 9.0% due to degradation of 1-(furan-2-yl)-2-hydroxyethanone in a zinc-chloride-rich environment. In his Ph.D. dissertation, Ni reported that cellulose can only be dissolved in aqueous zinc chloride between $R = 2.80$ and 4.26 hydrates.²² Other research similarly describes the solubility of cellulose in zinc chloride hydrates to be limited to between $R = 3.2$ and 3.3.^{17,20} Despite the considerable interest in zinc chloride hydrate as a solvent for cellulose, there is limited understanding of the solute–solvent interaction(s) that makes solubility possible. Using ¹H NMR spectroscopy and optical rotation measurements, Richards and Williams examined the solubility of several D-

Received: November 21, 2015

Revised: January 13, 2016

glucopyranosides to understand the complex formation between cellulose and zinc chloride.²⁴ Like cellulose, the model glucopyranosides exhibited a strong $\text{ZnCl}_2/\text{H}_2\text{O}$ concentration dependence on their solubility. Deviation in the chemical shift of both the anomeric and ring protons in the presence of zinc chloride suggested direct interaction of vicinal hydroxyl groups on C-2 and C-3 positions with the zinc.

We recently demonstrated that the $R = 3$ zinc chloride hydrate is best described as an ionic liquid (mp 6 °C) in which $[\text{Zn}(\text{OH}_2)_6][\text{ZnCl}_4]$ exhibits a CsCl-type packing of complex ions.²⁵ Furthermore, we have strong evidence for distinct ionic liquid structures at the $R = 9$ and 21 hydrates, with complete second and third water hydration shells, respectively, around the cationic zinc, charge balanced by the persistent $[\text{ZnCl}_4]^{2-}$ anion.²⁶ In the $R = 3$ hydrate, we recognize that the Zn^{2+} competes more effectively than the protons for the oxygen's charge density, making the system a strong hydrogen-bond donor. The Lewis acidity of Zn^{2+} further makes $[\text{ZnCl}_4]^{2-}$ a weak hydrogen bond acceptor. At the same time, neither molecular ion exhibits a dipole; thus, with the ionic packing requirement for three-dimensional charge cancelation, the $R = 3$ hydrate solvent is nonpolar. This structural description of a strong hydrogen-bond-donating but nonpolar solvent would seem ideally suited for dissolving cellulose, a nonpolar polymer with extensive intra- and intermolecular hydrogen bonding. We therefore initiated this study to articulate the solute–solvent interactions of cellulose in the zinc chloride hydrate system so as to understand its solubilization.

EXPERIMENTAL SECTION

Materials. Cellulose pulp was obtained from Whatman no. 1 filter paper. Anhydrous zinc chloride was obtained from Sigma Aldrich and heated in the oven (105 °C) overnight to remove residual water prior to use. Benzoyl chloride, pyridine, tetrahydrofuran, and sodium hydroxide were obtained from Sigma Aldrich and used without further purification. Deionized water was used to prepare the zinc chloride solution. D_2O and d^6 -ethanol used in neutron scattering experiments were purchased from Aldrich or Cambridge Isotope Laboratories (CIL) and used without further purification.

Dissolution and Regeneration of Cellulose. Zinc chloride hydrate melts were prepared by mixing the anhydrous salt with the appropriate molar ratio of deionized water. To test solubility, a mass (1 wt %) of cellulose was added to approximately 2 mL of hydrate melt and incubated at 25 °C for 72 h with occasional vortexing. Insoluble cellulose residue was removed from the liquor, washed with an excess of deionized water (20 mL), and then freeze-dried prior to TGA analysis. Separately, excess deionized water was added to the supernatant of any samples with undissolved material to precipitate and recover any cellulose that may have dissolved. In all cases, the water wash was observed only to contain zinc chloride residue. With no detectible cellulose, we assume that 100% of the cellulose precipitates.

To determine the influence of the hydrate melt solvent on the cellulose regenerated from solution, a parallel series of solutions of 0.5 wt % cellulose in the $R = 3$ hydrate, 1 mL each, were prepared and incubated at 25 °C for 12, 24, 48, 72, and 96 h with occasional vortexing. At this composition, the cellulose completely dissolves. Cellulose was then regenerated from the solutions by addition of excess deionized water (20 mL) as the precipitation solvent. The precipitate was then washed 10 times with 20 mL aliquots of deionized water followed by 5 washes

with 20 mL of a 1 wt % solution of sodium hydroxide to remove the remaining zinc chloride. Regenerated cellulose was freeze-dried for TGA and GPC analysis.

Thermogravimetric Analysis (TGA). A measure of the purity and integrity of the cellulose samples after regeneration from zinc chloride hydrates was determined using a TA Instruments TGA500, heating samples from 40 to 600 °C at 10 °C/min under nitrogen purge. All TGA plots were normalized to 100 wt % at 100 °C to account for minor variation of ambient moisture adsorbed to the cellulose.

Gel Permeation Chromatography (GPC). To perform GPC analyses, samples of cellulose were benzoylated to achieve solubility in conventional solvents using a previously established procedure with minor modifications.²⁷ Regenerated cellulose (20 mg) was dissolved in 1-allyl-3-methylimidazolium chloride (Amin chloride) (750 mg) in a 15 mL flask by first thoroughly dispersing the sample through vortexing, followed by heating at 80 °C for 3 h with magnetic stirring. After the solution became transparent, pyridine (250 μL , 2.8 mmol) was added, and the mixture was homogenized to form a uniform paste before being allowed to cool to room temperature. Benzoyl chloride (250 μL , 2.2 mmol) was added, and the sample was subsequently stirred for 3 h at 25 °C. The benzoylated product was precipitated by addition of a 1:3 mixture of deionized water and ethanol with vigorous stirring for 5 min. The collected white precipitate was washed several times with methanol to remove the trace amount of ionic liquid present and then dried at 70 °C under vacuum.

GPC analyses were carried out using a Waters model ALC/GPC 204 (Waters Associates, Milford, MA) and a Waters 510 pump equipped with a UV detector (210 nm). Standard monodisperse polystyrenes (molecular weight ranges from 0.82 to 1860 kg/mol) were used for calibration. A 1 mg/mL solution of the benzoylated cellulose in THF was injected into an Ultrastaygel column and eluted with THF at a 6 mL/min flow rate. The analysis was conducted at 35 °C. Standard monodisperse polystyrenes (molecular weight ranges from 0.82 to 1860 kg/mol) were used for calibration. The number (\bar{M}_n) and weight (\bar{M}_w) average molecular weights were calculated using the Millenium 32 software.

Turbidimetric Titration. A light scattering instrument was constructed to conduct turbidimetric titrations; a schematic is given in Supporting Information Figure S1. Here, a 20 mL sample holder, illuminated with diffuse white light, is inserted into the photodynamic cell such that light scattered by any precipitate can be measured as a voltage from a THORlabs DET210 photodetector. The voltage signal was measured using an AKTAKOM AM-1118 PC Link multimeter.

Cellulose solutions with concentration between 0.025 and 0.2 wt % were prepared in the $R = 3$ zinc chloride hydrate melt. Solutions with \geq the 0.2 wt % cellulose became too viscous such that even gentle stirring with the magnetic stir bar caused significant fluctuations in the scattered light intensity. In a typical titration experiment, 2.00 g (10.6 mmol) of solution was placed in the sample holder of the above-described light scattering instrument. Deionized water was systematically added in 160 μL (0.0088 mmol) increments, with stirring. After sufficient water was added, precipitation ensued, resulting in increased turbidity, measured as a function of the amount of light scattered. Each titration was performed in triplicate, with the average response reported. To determine the baseline for the light scattering instrument, a control titration was performed diluting a neat sample of $R = 3$ hydrate. The

response of the control was subtracted from that of the cellulose solutions to determine the turbidimetric response.

Neutron Scattering. Samples (1 mL) of $\text{ZnCl}_2 \cdot 3\text{D}_2\text{O}$ (separately prepared with Aldrich or CIL D_2O in our laboratory at NCSU or at Oak Ridge National Laboratory, respectively.), 1 wt % cellulose in $\text{ZnCl}_2 \cdot 3\text{D}_2\text{O}$ (Aldrich), $\text{ZnCl}_2 \cdot 3(d^6\text{-EtOD})$, and 1 wt % $d^6\text{-EtOD}$ in $\text{ZnCl}_2 \cdot 3\text{D}_2\text{O}$ (CIL) were sealed into 5 mm fused silica NMR tubes (WILMAD). The samples as well as an empty NMR tube were mounted on the linear sample changer installed at the NOMAD diffractometer, Spallation Neutron Source, Oak Ridge National Laboratory.²⁸ The linear sample changer was operated under vacuum to reduce the background. The neutron event data were binned as a function of Q using a calibration derived from measurement of diamond powder, as described in ref 28, and normalized to the integrated proton charge accumulated on the neutron target. Measurements obtained from a 5.8 mm diameter vanadium rod were used for normalization of the sample data to a differential cross section. Data were collected at room temperature as the sum of three 20 min scans for each sample. The incoherent contribution to the scattering cross section was approximated by a pseudo-Voigt function. Data were collected to $Q_{\text{max}} = 50 \text{ \AA}^{-1}$. On the basis of the total scattering, the structure factor $S(Q)$ and reduced atomic pair distribution function (PDF) $G(r)$ were evaluated with $Q_{\text{max}} = 10, 15, 20, 30, 40,$ and 50 \AA^{-1} to determine the Q cutoff that exhibits all clearly discernible real pair correlations and minimizes artifacts of the Fourier transform, found to be 30 \AA^{-1} . Transformation of the data to obtain $S(Q)$ and its inverse Fourier transform $G(r)$ was performed using the NOMAD-SNS analysis suite of programs.

RESULTS

Dissolution of Cellulose in Aqueous Zinc Chloride.

Initial efforts to dissolve cellulose in zinc chloride hydrates with varying degrees of hydration demonstrated that while cellulose is soluble in the $R = 3$ hydrate, it is insoluble in both $R = 2.3$ and 4.8 hydrates, as seen in Figure 1, where fragments of

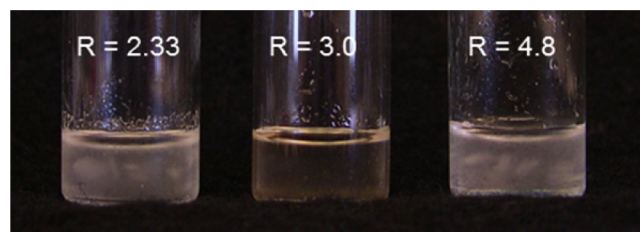


Figure 1. Photograph of the zinc chloride hydrates for which cellulose completely dissolves in the $R = 3$ hydrate but remains in suspension for the $R = 2.3$ and 4.8 hydrates.

cellulose filter paper are observed suspended in the solvent of the $R = 2.3$ and 4.8 hydrates but not the $R = 3.0$ hydrate. After 72 h in suspension at $25 \text{ }^\circ\text{C}$, the residual solid from the $R = 2.3$ and 4.8 hydrates was removed, thoroughly washed with deionized water, and freeze-dried. Separately, excess deionized water was added to the supernatant to precipitate any cellulose that may have dissolved; however, no precipitate was observed. TGA of cellulose recovered from $R = 2.3$ and 4.8 hydrates demonstrate a thermal decomposition profile similar to that of the original cellulose starting material, Figure 2.

Cellulose can be regenerated from $\text{ZnCl}_2 \cdot 3\text{H}_2\text{O}$ by addition of excess deionized water. The regenerated cellulose was

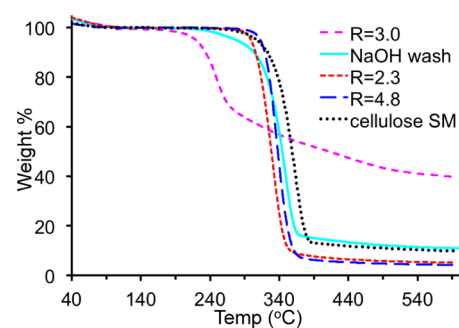


Figure 2. Thermogravimetric analyses of the cellulose starting material (black), recovered cellulose from the $\text{ZnCl}_2 \cdot \text{RH}_2\text{O}$ hydrates with $R = 2.3$ (red) and 4.8 (blue), the regenerated cellulose from $R = 3$ (magenta), and regenerated from $R = 3$ and washed with 1% NaOH solution (turquoise).

similarly washed 10 times with deionized water then freeze-dried. TGA of the regenerated cellulose in a nitrogen atmosphere (Figure 2) exhibits a substantially greater amount of residual ash upon decomposition than was observed for either the original starting material or the recovered cellulose from the $R = 2.3$ and 4.8 hydrates. This ash, likely zinc oxide/hydroxide/chloride, observed for cellulose samples even after extensive washing with deionized water, is indicative of strong interaction between the polymer and the zinc chloride hydrate. In addition, the cellulose regenerated from the $R = 3$ hydrate exhibits a two-step decomposition with an initial weight loss of about 30% starting at around $200 \text{ }^\circ\text{C}$, followed by additional weight loss to 42% of the initial weight by $500 \text{ }^\circ\text{C}$. The two weight loss steps for the regenerated material likely correspond to loss of waters of hydration from coordinated zinc chloride hydrate and combustion of the cellulose, respectively. The residual zinc chloride can be readily removed from the regenerated cellulose by additional washing with a 1 wt % aqueous NaOH solution. TGA of the NaOH washed regenerated cellulose is very similar to that of the original cellulose starting material, as shown in Figure 2 (and also Figure 6).

The above experiments, consistent with earlier literature reports,^{17,20–23} demonstrate that zinc chloride dissolves cellulose in only a narrow composition range of hydrate melts, specifically $3 - x < R < 3 + x$ with $x \approx 1$. However, as shown in the photograph of Figure 3, once dissolved, the cellulose stays in solution until a significant amount of water is added. To measure the hydrate composition at which cellulose precipitates, turbidimetric titrations were performed. As evident in Figure 4, an increase in scattered light, seen by the voltage from the photodiode, is observed starting after an additional 6

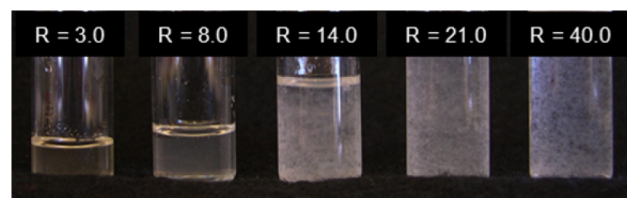


Figure 3. Photographs of samples with additional water added to 1 wt % cellulose dissolved in the $R = 3$ zinc chloride hydrate solvent. Cellulose remains in solution for days for the $R = 8$ hydrate but completely precipitates immediately upon addition of excess water, for example, $R = 14, 21,$ and 40 .

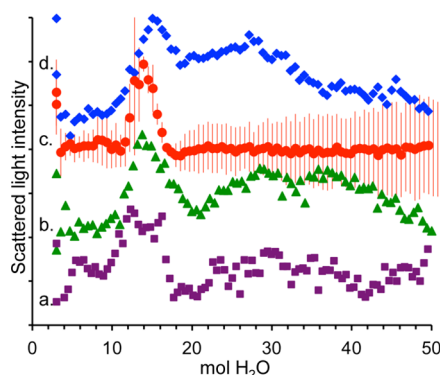


Figure 4. Turbidimetric titration of (a) 0.05, (b) 0.075, (c) 0.1, and (d) 0.2% cellulose dissolved in the $R = 3$ zinc chloride hydrate solvent. Error bars of ± 1 standard deviation for the average of three measurements are plotted for the 0.1% solution, which exhibited the most reasonable compromise between the amount of material and viscosity of the medium for the light scattering experiment. Errors are 2–3 times that magnitude for the other concentrations.

equiv. of water has been added to a net $R = 9$ hydrate composition. The onset of precipitation at the $R = 9$ composition is independent of the initial concentration of dissolved cellulose. Similarly, at all cellulose concentrations, the scattered light reaches a maximum between values of $R = 14$ – 15 , which is apparently the hydrate concentration at which precipitation is complete. With further addition of water, the amount of light scattered decreases, reaching a minimum near $R = 20$. Beyond $R = 20$, the light scattering may be indicative of additional flocculation.

Impact of the Zinc Chloride Hydrate on Cellulose. The zinc chloride hydrate is a significantly acidic solvent due to both the Lewis acidity of the Zn^{2+} and the Brønsted acidity of the coordinated water, which reasonably might be expected to break down cellulose. To investigate the stability of cellulose dissolved in the $R = 3$ hydrate, the GPC molecular weight and TGA analyses of samples aged in solution for up to 96 h at 25 °C, and then regenerated by water dilution and NaOH wash, were evaluated.

Due to the insolubility of the cellulose molecules in common organic solvents necessary for GPC measurements, the hydroxyl groups of the regenerated cellulose were benzoylated prior to analysis. GPC traces of the cellulose starting material and cellulose regenerated after incubation in the $R = 3$ zinc chloride hydrate melt are given in Figure 5. The number average molecular weight (\bar{M}_n), weight average molecular weight

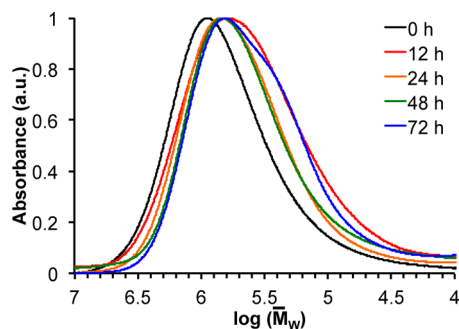


Figure 5. GPC traces of cellulose regenerated from the $R = 3$ zinc chloride hydrate solution after definite incubation time intervals, compared to cellulose starting material.

weight (\bar{M}_w), and the distribution of molecular weight (\bar{M}_w/\bar{M}_n) were calculated from the GPC data and are reported in Table 1. There is minimal breakdown of the cellulose

Table 1. Molecular Weights of the Regenerated Cellulose from Zinc Chloride Hydrate as a Function of Time

time (h)	\bar{M}_w (KD)	\bar{M}_n (KD)	\bar{M}_w/\bar{M}_n
0	1200	500	2.4
12	1000	445	2.47
24	880	265	2.80
48	810	244	3.32
72	760	214	3.58

polymer after 12 h in solution. However, the molecular weight distribution of the regenerated cellulose shifts toward lower molecular weight and greater polydispersity with increased time in the hydrate melt solution. The Lewis acidic character of zinc chloride is likely responsible for any chain scission of the cellulose molecules, albeit the OH stretch in H_2O (3362 cm^{-1}) compared to that in $[\text{Zn}(\text{OH}_2)_6][\text{ZnCl}_4]$ (3414 cm^{-1}) demonstrates that this is not a strongly acidic solvent.²⁵

TGA traces of cellulose samples regenerated (including NaOH wash) after incubation at 25 °C for 0–96 h in the $R = 3$ hydrate solution are given in Figure 6. The general character-

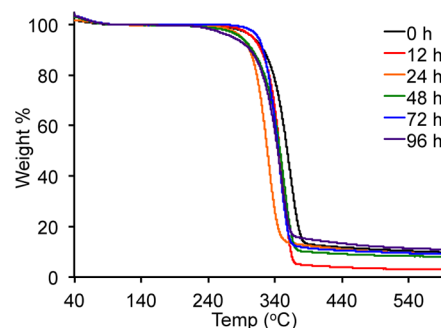


Figure 6. TGA traces of cellulose regenerated from the $R = 3$ zinc chloride hydrate solution after definite incubation time intervals, compared to cellulose starting material.

istics of the thermal degradation of the pure cellulose and the regenerated samples from the zinc chloride hydrate solution are consistent for all samples. Some variation in the temperature of onset of thermal decomposition is observed. These results demonstrate that cellulose regenerated from the hydrate solution exhibits minimally decreased thermal stability as compared to the cellulose starting material. Notably, there is no systematic trend observed relating the temperature of decomposition to the duration of incubation in zinc chloride hydrate solution, in contrast with the previously mentioned molecular weight analyses.

Neutron Scattering of Solution Structure. Having established the $R = 3$ hydrate to be an ionic liquid $[\text{Zn}(\text{OH}_2)_6][\text{ZnCl}_4]$,²⁵ a series of neutron scattering studies were pursued to further decipher structural details of the cellulose/zinc chloride hydrate solution. Room-temperature neutron structure factor, $S(Q)$, and PDF, $G(r)$, data for these solutions are given in Figure 7. An important question to resolve is whether the cellulose is bound directly to the zinc or whether cellulose exhibits only outer-sphere interactions with the solvent. Because ZnCl_2 is also highly soluble in ethanol, we

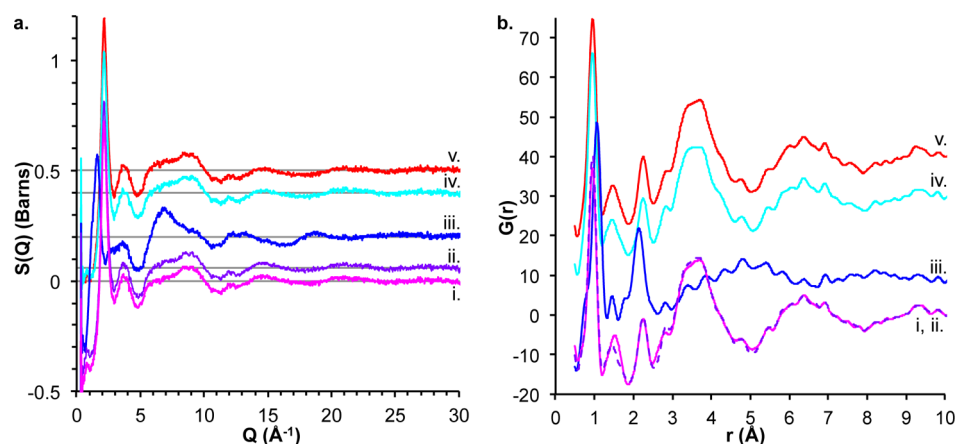


Figure 7. Neutron scattering (a) structure factor and (b) PDF data for (i) $\text{ZnCl}_2 \cdot 3\text{D}_2\text{O}$ (Aldrich) (magenta), (ii) $\text{ZnCl}_2 \cdot 3\text{D}_2\text{O}$ (CIL) (purple), (iii) $\text{ZnCl}_2 \cdot 3 d^6\text{-EtOD}$ (blue), (iv) 1 wt % $d^6\text{-EtOD}$ in $\text{ZnCl}_2 \cdot 3\text{D}_2\text{O}$ (CIL) (turquoise), and (v) 1 wt % cellulose in $\text{ZnCl}_2 \cdot 3\text{D}_2\text{O}$ (Aldrich) (red).

utilized the $R = 3$ ethanol solution as a reference to structural features that differentiate alcohol from water inner-sphere coordination to zinc. Presumably, ethanol coordinated to zinc could serve as a reasonable model of a primary OH group of cellulose bound to zinc. Thus, neutron scattering data were collected for the $R = 3$ $d^6\text{-EtOD}$ solution, as well as for solutions with 1 wt % cellulose or 1 wt % ethanol dissolved in the $R = 3$ D_2O hydrate (approximately 1 mol cellulose/60 mol $\text{ZnCl}_2 \cdot 3\text{D}_2\text{O}$ and 1 mol ethanol:/20 mol $\text{ZnCl}_2 \cdot 3\text{D}_2\text{O}$, respectively, to keep the hydrocarbon solute content approximately equivalent).

Two data sets for the $R = 3$ hydrate prepared with D_2O purchased from Aldrich and CIL were measured. The structure factor and PDF data for these are consistent with that previously reported,²⁵ with the minor variation in the PDF intrawater D–D contacts at about 1.5 Å and Zn–D, D–O, D–Cl, and D–D contacts at around 2.4–2.8 Å likely being reflective of minor differences in the H/D isotopic purity of the water. The 1 wt % cellulose solution was prepared using the Aldrich D_2O , whereas the 1 wt % ethanol solution was prepared using the CIL D_2O . With only 1 wt % of cellulose or ethanol dissolved in the $R = 3$ hydrate solution, very little variation in the structure factor $S(Q)$ is observed for the solutions. Slight but significant variation, however, is observed by differential PDF analysis (i.e., solution–solvent), as will be described in detail in the Discussion section.

A thorough structural study of $\text{ZnCl}_2 \cdot 3$ ethanol is in progress and will be the subject of a future report. However, here, we note the similarity between the $R = 3$ D_2O and $R = 3$ $d^6\text{-EtOD}$ solutions, with peaks observed in the structure factor of the latter being shifted to lower Q , consistent with an expanded structure but in keeping with an ionic liquid model that we propose to be $[\text{Zn}(\text{OEt})_6][\text{ZnCl}_4]$. Specifically, the principle peak at 2.14 \AA^{-1} in the hydrates is shifted to 1.62 \AA^{-1} in the ethanol solution, with a significant shoulder on the low Q side of the peak. We suspect the ethanol solution also exhibits a so-called first sharp diffraction peak, the analogue of the peak at 0.8 \AA^{-1} in the hydrate, but at lower Q , below the limit of the current detectors.

Even the simple hydrocarbon arm of ethanol adds a large number of pair correlations to the PDF, as observed in Figure 7b. To help decipher these contacts, the data are compared with the distances reported for the neutron scattering of pure ethanol²⁹ and with respect to distances from the reported

crystal structure of $[\text{Zn}(\text{OEt})_6][\text{ClO}_4]_2$.³⁰ That structural data is schematically summarized in Figure 8, for which

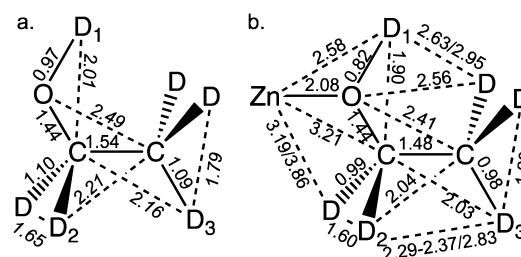


Figure 8. Diagram of pair correlations from (a) the liquid structure of ethanol (ref 29) and (b) for ethanol coordinated to zinc in $[\text{Zn}(\text{OEt})_6][\text{ClO}_4]_2$ (ref 30).

reported distances reasonably correspond to the $<4 \text{ \AA}$ pair correlations of the experimental PDF in Figure 7b. Interestingly, the low r shoulder on the $G(r)$ peak at around 1 Å is consistent with O–D distances being slightly shorter than C–D distances. Notably too, the pair correlation at 2.25 Å, corresponding to Zn–O and Zn–Cl contacts in the $R = 3$ hydrate, is shifted to 2.14 Å in the $R = 3$ ethanol solution because of the addition of numerous two-bond C–D contacts of similar distance. Of particular interest to this current study are the three peaks at 2.82, 3.38 (with a shoulder at 3.1 Å), and 3.85 Å. On the basis of the crystal structure of $[\text{Zn}(\text{OEt})_6][\text{ClO}_4]_2$,³⁰ these are reasonably assigned as correlations unique to alcohol coordination including three-bond D–D (2.8 Å), two-bond Zn–C (3.2 Å), and three-bond Zn–D (3.2 and 3.9 Å), as well as interligand C–O (3.3–3.4 and 3.9 Å), D–O (2.8 and 3.2–2.3 Å), and C–D (3.2 and 3.7 Å).

DISCUSSION

That cellulose dissolves in the $R = 3$ hydrate of zinc chloride has been known at least since its report in an 1859 English patent.¹⁸ Nevertheless, the intermolecular characteristics necessary to achieve solubilization of this complex biopolymer in the zinc chloride hydrate melt have yet to be articulated.

Our present and others' previous literature reports^{17,20–23} clearly demonstrate that there is only a narrow extent-of-hydration window around $R = 3$ that affords the necessary solubilization characteristics. That cellulose solubility is not observed in the most unsaturated zinc chloride molten hydrates

(at 20 °C, the composition of a saturated solution is $R = 1.9$) argues against direct coordination between cellulose hydroxyls and the Zn^{2+} . However, as demonstrated in this report, zinc chloride is precipitated along with the cellulose when regenerated from the zinc chloride hydrate solution. The zinc chloride is only displaced by addition of a more strongly coordinating hydroxyl, here, 1 wt % NaOH, which argues for the existence of direct cellulose–Zn coordination.

As shown by GPC and TGA analyses, cellulose regenerated from the zinc chloride hydrate melt is broken down to somewhat lower molecular weight fractions with increased time in the zinc chloride hydrate solution. The Lewis acidity of Zn^{2+} is anticipated to facilitate the cleavage of glycosidic linkages of cellulose, where protonation of the glycosidic oxygen is followed by elimination and charge stabilization of the ensuing carbocation at the anomeric center as facilitated by an oxonium–cation resonance stabilization mechanism. This is similar to the observations of Lu and Shen who worked with bacterial cellulose.²⁹ Nevertheless, the fact that the cellulose polymer remains largely intact through the dissolution/regeneration process indicates that the cellulose polymer itself, not just decomposed fragments, is soluble in the $R = 3$ zinc chloride hydrate melt.

It is striking that while hydrate melts with more than about 4 equiv. of water do not dissolve cellulose, the turbidimetric titration data demonstrate that once dissolved, the cellulose remains in solution until the $R = 9$ level of hydration, with complete precipitation occurring by the $R = 15$ hydration level. This indicates that distinct chemistries are required to dissolve cellulose than are necessary to keep it in solution once dissolved. Presumably, initial solubilization requires the solvent to break the extensive hydrogen bonding network of solid cellulose. Once the hydrogen bond network is broken, different chemical interactions may keep the less condensed form of the polymer in solution.

As described in the Introduction, we suggest that the ionic liquid structure of the $R = 3$ zinc chloride hydrate melt, $[\text{Zn}(\text{OH}_2)_6][\text{ZnCl}_4]$, which is nonpolar but a strong hydrogen bond donor,²⁵ may account for its ability to dissolve cellulose. While not precluding direct coordination to zinc, the strong hydrogen bond donor ability of the first coordination shell of water in the ionic liquid structure is apparently critical for cellulose solubility because solubilization is only achieved when the first hydration shell is complete, or nearly so, at the $R = 3$ composition. Strong hydrogen bonding interactions of first coordination shell water to the hydroxyls of glucopyranosides or cellulose can account for the reported deviation in the ^1H NMR chemical shift for both anomeric and ring protons when dissolved in the zinc chloride hydrate equivalently to the previously proposed model, which suggested direct interaction of vicinal hydroxyl groups on C-2 and C-3 positions with zinc.²⁴

Additional waters of hydration dramatically change the structure and thus the solubilizing characteristics of hydrate melts. Raman spectroscopy demonstrates that the $[\text{ZnCl}_4]^{2-}$ anion persists to high levels of dilution ($R > 100$).²⁶ Correspondingly, DSC, diffraction, and IR spectroscopy studies indicate that the further hydration results in ionic liquid structures for which the cation is enlarged with additional hydration spheres around the cationic zinc.²⁶ A second hydration shell is complete at the $R = 9$ hydrate composition, $[\text{Zn}(\text{OH}_2)_6(\text{OH}_2)_{12}][\text{ZnCl}_4]$, and a third hydration shell is complete at the $R = 21$ hydrate composition, $[\text{Zn}(\text{OH}_2)_6(\text{OH}_2)_{12}(\text{OH}_2)_{24}][\text{ZnCl}_4]$. In the dilute hydrate melts

with higher-level hydration shells, there is a much greater extent of intrasolvent hydrogen bonding, which makes them inferior hydrogen bond donor solvents than the $R = 3$ hydrate. We suggest that this accounts for the inability of higher hydrates to dissolve cellulose.

Notably, once dissolved, cellulose remains in solution until the $R = 9$ hydrate composition is achieved, coincident with the composition of a complete second hydration shell. As shown in Figure 4, as well as visually for 1 and 2% cellulose solutions (the latter being too viscous for effective turbidimetric measurements with our constructed device), the onset of precipitation at the $R = 9$ composition is independent of the amount of dissolved cellulose, thus demonstrating that the nature of the solvent and not the concentration of solute governs this solubility. The turbidimetric titration also demonstrates that precipitation is complete at about the $R = 15$ hydrate composition. These data suggest that for solubilization, cellulose must be associated to the first hydration shell through hydrogen bonding while also gaining solute/solvent stabilization by becoming part of higher hydration shells. Once there is sufficient water present to completely fill the second hydration shell, the hydroxyls of cellulose are less energetically favored than water to be incorporated into the hydrate melt's ionic liquid structure. Above this hydrate composition, cellulose–cellulose hydrogen bonding is more energetically favored than cellulose to second- and third-shell water hydrogen bonding, thus resulting in precipitation.

While the above data clearly indicate that the hydration shells of the zinc chloride hydrate melt are critical for cellulose solubilization, the data neither support or refute whether or not direct coordination between cellulose hydroxyls and the Zn^{2+} occurs. We thus turned to total neutron scattering and corresponding PDF analysis in search of evidence of direct zinc cellulose coordination based on pair correlations unique to alcohol coordination. Utilizing differential PDF analysis to compare the structure of the solution and pure solvent, it is possible to subtract the solvent zinc–water and $[\text{ZnCl}_4]^{2-}$ pair correlations from the solution in order to probe unique solute–solvent interactions. Furthermore, we utilize ethanol, which we propose also forms an ionic liquid at the $R = 3$ composition, as a simple model system to decipher possible pair correlations resulting from zinc interacting with primary OH functional groups of cellulose. Differential PDF plots of the difference between the $R = 3$ d^6 -EtOD and $R = 3$ D_2O ionic liquids and for solutions with 1 wt % d^6 -EtOD or 1 wt % protonated cellulose dissolved in the $R = 3$ D_2O zinc chloride hydrate melt with respect to the neat $R = 3$ solvent are shown in Figure 9.

We preface discussion of the differential PDF assignments with a caution of overinterpretation of the PDF data, particularly in systems such as this with many overlapping pair correlations. Nevertheless, the consistency of peak assignments between these three systems, as well as with PDF analyses based on Q_{max} cutoffs ranging from 10 to 50 \AA^{-1} to differentiate peaks that are real from those that are Fourier effects, gives confidence that our interpretation of the data is reasonable.

Because each ethanol ligand brings five C–D contacts, which are slightly longer than the single O–D contact, as opposed to only two O–D contacts for each water, the difference PDF at around 1 \AA for $[(R = 3 \text{ ethanol}) - (R = 3 \text{ water})]$ exhibits a derivative-type pattern resulting from the pair correlation being shifted to larger r . The pair correlation at 1.45 \AA is indicative of the O–C and C–C contacts present in ethanol. The difference

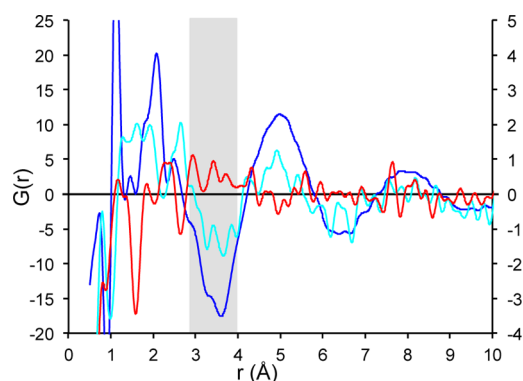


Figure 9. Differential PDF plots of $[(R = 3 \text{ } d^6\text{-EtOD}) - (R = 3 \text{ D}_2\text{O(CIL)})]$ (blue) and, on the $5\times$ expanded scale (right), $[(1 \text{ wt } \% \text{ } d^6\text{-EtOD in } R = 3 \text{ D}_2\text{O(CIL)}) - (R = 3 \text{ D}_2\text{O(CIL)})]$ (turquoise) and $[(1 \text{ wt } \% \text{ cellulose in } R = 3 \text{ D}_2\text{O(Aldrich)}) - (R = 3 \text{ D}_2\text{O(Aldrich)})]$ (red). Peaks in the shaded region are assigned to direct zinc–alcohol coordination.

shoulder at 1.9 Å and the peak at 2.1 Å is indicative of two-bond intramolecular D–D and D–C contacts, and the peak at ~ 2.4 Å is consistent with two-bond O–C and three-bond D–D and O–D contacts. The alternating negative and positive features in the differential PDF at about 3.5, 5, 6.5, and 8 Å are a result of intermolecular ion contacts, with the pattern being a result of the difference in size between $[\text{Zn}(\text{OD}_2)_6]^{2+}$ and $[\text{Zn}(\text{ODC}_2\text{D}_5)_6]^{2+}$ molecular cations. The shoulders on the 3.5 Å negative difference peak at 2.9, 3.4, and 3.9 Å are a result of the three peaks, noted in the results description of the $R = 3$ ethanol solution to be indicative of two-bond Zn–C, three-bond Zn–D, as well as D–O, C–O, and C–D contacts between neighboring ligands, all of which are unique to direct zinc–alcohol coordination.

With only 1 wt % ethanol dissolved in the $R = 3$ zinc chloride hydrate solvent, pair correlations corresponding to ethanol as the solute are less pronounced in the differential PDF plot and hence are plotted on a $5\times$ scale in Figure 9. Nevertheless, essentially all of the pair correlations assigned from the above comparison of the neat $R = 3 \text{ } d^6\text{-EtOD}$ and $R = 3 \text{ D}_2\text{O}$ hydrate melts are again identified in the 1 wt % ethanol solution. In fact, the features argued to be indicative of two-bond Zn–C, three-bond Zn–D, and interligand D–O, C–O, and C–D contacts, which are unique to direct zinc–alcohol coordination, are more clearly discernible.

Conducting the neutron scattering experiment with 1 wt % protonated cellulose adds an additional challenge because of the negative scattering length of H (-3.74 fm) relative to D (6.67 fm). While hydroxyl protons undoubtedly will exchange with water deuterons, the hydrocarbon protons of cellulose should remain protonated. This is consistent with the negative peaks in the $[(1 \text{ wt } \% \text{ cellulose}) - (R = 3 \text{ D}_2\text{O})]$ difference PDF at 1.6 and 2.6 Å, assigned as two-bond H \cdots H and three-bond H \cdots H, H \cdots C, and H \cdots O contacts, respectively. Most importantly with respect to this study, however, the peaks at 2.9, 3.4, and 3.7 Å, analogous to the above zinc–ethanol assignments, are indicative of direct coordination of cellulose primary O(H/D) to zinc.

Together, all of the above data lead us to propose a structural model, diagrammed in Figure 10, for the cellulose solute in the ionic liquid $R = 3$ zinc chloride hydrate solvent. Here, the primary OH functional group of cellulose is directly coordinated to zinc, along with five additional waters of

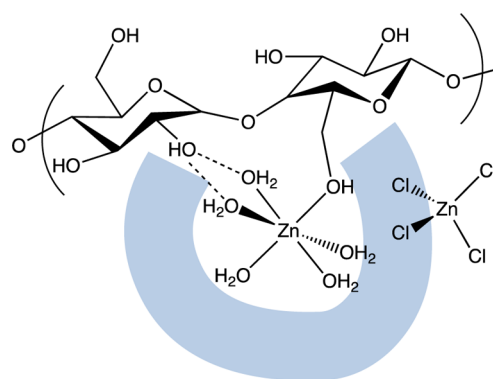


Figure 10. Schematic of the proposed interaction between the cellulose solute and the zinc chloride hydrate around zinc after which point additional water results in cellulose precipitation.

hydration to fill the first hydration shell. The ring hydroxyls then likely participate as part of a second hydration shell, hydrogen bonded to the strong hydrogen bond donor first-shell water molecules.

On the basis of this model, if there is no access for the primary OH functional group to become part of the first hydration shell, that is, quantities of water much beyond $R = 3$, or there are not sufficient waters to complete the remainder of the first hydration shell such that the remainder of the cellulose hydroxyls can participate in the second hydration shell, that is, quantities of water much less than $R = 3$, then cellulose will not be dissolved by the zinc chloride hydrate. However, once in solution, this model suggests that cellulose solubility remains possible until sufficient water is added to completely fill the solvent's second hydration shell. The shaded blue curve cartoons a second hydration shell around the hydrated zinc cation.

CONCLUSION

Long known to solubilize cellulose, the recently discovered ionic liquid nature of the $R = 3$ zinc chloride hydrate melt, better formulated as $[\text{Zn}(\text{OH}_2)_6][\text{ZnCl}_4]^{25}$ reveals the molecular interactions responsible for its remarkable solubility characteristics. As an ionic liquid with nonpolar ions and the water ligands coordinated to the Lewis acidic zinc but with the weak $[\text{ZnCl}_4]^{2-}$ as the only hydrogen bond acceptor, this hydrate melt is a nonpolar, strongly hydrogen bond donating solvent, ideally suited for solubilizing cellulose. Molecular weight determination as well as thermal degradation studies demonstrates that while the cellulose dissolved in the $R = 3$ zinc chloride hydrate is slightly broken down with time in solution, the intact cellulose polymer, not just decomposed fragments, is soluble in this unique solvent.

Results reported here confirm previous reports that cellulose is dissolved in hydrate melts only within a narrow hydration window of $3 - x < R < 3 + x$, with $x \approx 1$.^{17,20–23} In addition, it is demonstrated that once in solution, cellulose remains dissolved over the hydrate composition range $3 < R < 9$. Notably, the hydrate composition at which cellulose precipitation initiates coincides with the composition at which a second hydration shell around the hydrated zinc cation is complete. Neutron scattering and corresponding differential PDF analysis provide strong evidence that in solution, there is also direct coordination of the cellulose primary OH groups to the cationic zinc. Together, these data point toward a

solubilization model in which the primary OH groups of cellulose directly coordinate to zinc, participating in the first coordination shell of the ionic liquid's molecular cation. Ring hydroxyls of cellulose then become part of higher coordination shells around the molecular cation. If sufficient water is present to complete both first and second hydration shells around the cationic zinc, then cellulose begins to precipitate. With the additional water, cellulose hydroxyls can access neither direct coordination to zinc nor the strong hydrogen bond donors of first coordination shell water, precluding solubility.

■ ASSOCIATED CONTENT

Supporting Information

The Supporting Information is available free of charge on the ACS Publications website at DOI: 10.1021/acs.jpcc.5b11400.

Figure S1 describes the light scattering, turbidimetric titration apparatus (PDF)

■ AUTHOR INFORMATION

Corresponding Author

*E-mail: Jim_Martin@ncsu.edu

Notes

The authors declare no competing financial interest.

■ ACKNOWLEDGMENTS

This work was supported by NSF Grant DMR-0705190. Research conducted at ORNL's Spallation Neutron Source was sponsored by the Scientific User Facilities Division, Office of Basic Energy Sciences, U.S. Department of Energy (DOE), with assistance from Dr. Jörg Neufeind, Dr. Mikhail Feygenson, and John Carruth.

■ REFERENCES

- (1) Pinkert, A.; Marsh, K. N.; Pang, S. Reflections on the Solubility of Cellulose. *Ind. Eng. Chem. Res.* **2010**, *49*, 11121–11130.
- (2) Pinkert, A.; Marsh, K. N.; Pang, S.; Staiger, M. P. Ionic Liquids and their Interaction with Cellulose. *Chem. Rev.* **2009**, *109*, 6712–6728.
- (3) *Cellulose Solvents: For Analysis, Shaping and Chemical Modification*; Liebert, T. F., Heinze, T. J., Edgar, K. J., Eds.; American Chemical Society: Washington, DC, 2009.
- (4) Van de Vyver, S.; Geboers, J.; Jacobs, P. A.; Sels, B. F. Recent Advances in the Catalytic Conversion of Cellulose. *ChemCatChem* **2011**, *3*, 82–94.
- (5) Sen, S.; Martin, J. D.; Argyropoulos, D. S. Review of Cellulose Non-Derivatizing Solvent Interactions with Emphasis on Activity in Inorganic Molten Salt Hydrates. *ACS Sustainable Chem. Eng.* **2013**, *1*, 858–870.
- (6) Short, R. D.; Munro, H. S. Conclusions Drawn From a Study of Cellulose Nitration in Technical Mixed Acids by X-ray Photoelectron Spectroscopy and ^{13}C Nuclear Magnetic Resonance. *Polymer* **1993**, *34*, 2714–2719.
- (7) Padhye, M. R.; Deshpande, M. M. Cellulose Degradation in Xanthate Process. *J. Appl. Polym. Sci.* **1988**, *36*, 1475–1478.
- (8) Ratanakamnuan, U.; Atong, D.; Aht-Ong, D. Cellulose Esters from Waste Cotton Fabric via Conventional and Microwave Heating. *Carbohydr. Polym.* **2012**, *87*, 84–94.
- (9) Fujimoto, T.; Takahashi, S. I.; Tsuji, M.; Miyamoto, T.; Inagaki, H. Reaction of Cellulose with Formic Acid and Stability of Cellulose Formate. *J. Polym. Sci., Part C: Polym. Lett.* **1986**, *24*, 495–501.
- (10) Takahashi, S. I.; Fujimoto, T.; Barua, B. M.; Miyamoto, T.; Inagaki, H. ^{13}C NMR Spectral Studies on the Distribution of Substituents in Some Cellulose Derivatives. *J. Polym. Sci., Part A: Polym. Chem.* **1986**, *24*, 2981–2993.
- (11) Nehls, I.; Wagenknecht, W.; Philipp, B.; Stscherbina, D. Characterization of Cellulose and Cellulose Derivatives in Solution by High Resolution ^{13}C NMR Spectroscopy. *Prog. Polym. Sci.* **1994**, *19*, 29–78.
- (12) Fox, S. C.; Li, B.; Xu, D.; Edgar, K. J. Regioselective Esterification and Etherification of Cellulose: A Review. *Biomacromolecules* **2011**, *12*, 1956–1972.
- (13) Armand, M.; Endres, F.; MacFarlane, D. R.; Ohno, H.; Scrosati, B. Ionic-liquid Materials for the Electrochemical Challenges of the Future. *Nat. Mater.* **2009**, *8*, 621–629.
- (14) Braunstein, J. Some Aspects of Solution Chemistry in Liquid Mixtures of Inorganic Salts with Water. *Inorg. Chim. Acta, Rev.* **1968**, *2*, 19–30.
- (15) Leipner, H.; Fischer, S.; Brendler, E.; Voigt, W. Structural Changes of Cellulose Dissolved in Molten Salt Hydrates. *Macromol. Chem. Phys.* **2000**, *201*, 2041–2049.
- (16) Fischer, S.; Leipner, H.; Thümmel, K.; Brendler, E.; Peters, J. Inorganic Molten Salts as Solvents for Cellulose. *Cellulose* **2003**, *10*, 227–236.
- (17) Cao, N. J.; Xu, Q.; Chen, C. S.; Gong, C. S.; Chen, L. F. Cellulose Hydrolysis Using Zinc-Chloride as a Solvent and Catalyst. *Appl. Biochem. Biotechnol.* **1994**, *45–64*, 521–530.
- (18) Taylor, T. Improved Means of Giving Increased Strength to Paper, English Patent 787, 1859.
- (19) Cao, N. J.; Xu, Q.; Chen, L. F. Acid-hydrolysis of Cellulose in Zinc-chloride Solution. *Appl. Biochem. Biotechnol.* **1995**, *51–52*, 21–28.
- (20) de Almeida, R. M.; Li, J. R.; Nederlof, C.; O'Connor, P.; Makkee, M.; Moulijn, J. A. Cellulose Conversion to Isosorbide in Molten Salt Hydrate Media. *ChemSusChem* **2010**, *3*, 325–328.
- (21) Yang, L.; Li, G.; Yang, F.; Zhang, S.-M.; Fan, H.-X.; Lv, X.-N. Direct Conversion of Cellulose to 1-(furan-2-yl)-2-hydroxyethanone in Zinc Chloride Solution Under Microwave Irradiation. *Carbohydr. Res.* **2011**, *346*, 2304–2307.
- (22) Ni, J. Structure and Applications of Cellulose Regenerated from Zinc-cellulose Complexes, Thesis, Purdue University, West Lafayette, IN, 1999.
- (23) Lu, X.; Shen, X. Solubility of Bacteria Cellulose in Zinc Chloride Aqueous Solutions. *Carbohydr. Polym.* **2011**, *86*, 239–244.
- (24) Richards, N. J.; Williams, D. G. Complex Formation Between Aqueous Zinc Chloride and Cellulose Related D-Glucopyranosides. *Carbohydr. Res.* **1970**, *12*, 409–420.
- (25) Wilcox, R. J.; Losey, B. P.; Folmer, J. C. W.; Martin, J. D.; Zeller, M.; Sommer, R. Crystalline and Liquid Structure of Zinc Chloride Trihydrate: A Unique Ionic Liquid. *Inorg. Chem.* **2015**, *54*, 1109–1119.
- (26) Wilcox, R. J. Sorption to Dissolution: The Reactivity of Small Molecules with Condensed Phase Metal Halide Networks, Thesis, North Carolina State University, Raleigh, NC, 2009.
- (27) Zoia, L.; King, A. W. T.; Argyropoulos, D. S. Molecular Weight Distributions and Linkages in Liganocellulosic Materials Derived from Ionic Liquid Media. *J. Agric. Food Chem.* **2011**, *59*, 829–838.
- (28) Neufeind, J.; Feygenson, M.; Carruth, J.; Hoffmann, R.; Chipley, K. The Nanoscale Ordered Materials Diffractometer NOMAD at the Spallation Neutron Source SNS. *Nucl. Instrum. Methods Phys. Res., Sect. B* **2012**, *287*, 68–78.
- (29) Benmore, C. J.; Loh, Y. L. The Structure of Liquid Ethanol: A Neutron Diffraction and Molecular Dynamics Study. *J. Chem. Phys.* **2000**, *112*, 5877–5883.
- (30) Sudbrake, C.; Müller, B.; Vahrenkamp, H. Hexakis(alcohol)zinc Complexes. *Eur. J. Inorg. Chem.* **1999**, *1999*, 2009–2012.